Position swapping and pinching in Bose-Fermi mixtures with two-color optical Feshbach resonances

S. Gautam,[1] P. Muruganandam,[2] and D. Angom[1]
[1]*Physical Research Laboratory, Navarangpura, Ahmedabad 380 009, India*
[2]*School of Physics, Bharathidasan University, Tiruchirapalli 620 024, Tamil Nadu, India*
(Received 13 November 2010; published 10 February 2011)

We examine the density profiles of the quantum degenerate Bose-Fermi mixture of ^{174}Yb-^{173}Yb, experimentally observed recently, in the mean-field regime. In this mixture there is a possibility of tuning the Bose-Bose and Bose-Fermi interactions simultaneously using two well-separated optical Feshbach resonances, and it is a good candidate to explore phase separation in Bose-Fermi mixtures. Depending on the Bose-Bose scattering length $a_{\rm BB}$, as the Bose-Fermi interaction is tuned the density of the fermions is pinched or swapping with bosons occurs.

DOI: 10.1103/PhysRevA.83.023605 PACS number(s): 03.75.Hh, 67.85.Pq

I. INTRODUCTION

The quantum degeneracy in a boson-Fermi mixture was first experimentally realized for the system consisting of ^{7}Li and ^{6}Li [1,2]. Since then it has been observed in several other Bose-Fermi mixtures, ^{23}Na-^{6}Li [3], ^{87}Rb-^{40}K [4], ^{87}Rb-^{6}Li [5], ^{4}He-^{3}He [6], ^{174}Yb-^{173}Yb [7], and ^{84}Sr-^{87}Sr [8]. These are candidate systems to explore the effects of boson-induced fermionic interactions; of particular interest is the boson-mediated fermionic superfluidity. Another property of interest is the dynamical instabilities of the fermionic component arising from the attractive fermionic interactions, which is also boson mediated [9]. Precondition to observe either of these is a precise control of the interspecies interaction through a Feshbach resonance. This has been observed in ^{87}Rb-^{40}K [10,11] and used to trigger the dynamical collapse of ^{40}K [9]; the same is numerically analyzed in Refs. [12,13]. A similar setup is suitable to create fermionic ultracold molecules and was theoretically analyzed in a recent work [14].

Density distributions in the phase-separated domain of the Bose-Fermi mixture is also an important property of interest. Like in binary condensates, dynamical instabilities can be initiated in the phase-separated domain through manipulations of interaction strengths. For binary condensates, the recent work on mixtures of two different hyperfine states of ^{87}Rb [15] is a fine example of controlled experiment on phase separation.

In this regard, Molmer and collaborator [16,17] examined the zero-temperature equilibrium density distributions and predicted widely varying density patterns as a function of interspecies interactions. However, the Bose-Bose and Bose-Fermi interactions considered are extremely strong for experimental realizations. Similar studies have examined the ground-state geometry in spherical traps [18,19]. The conditions for mixing-demixing have been analyzed for homogeneous Bose-Fermi mixtures [20] and Bose-Fermi mixtures inside traps [18,21]. Although very high interaction strengths are achievable through magnetic Feshbach resonances in alkali-metal atoms, simultaneous tuning of both the boson-boson and boson-fermion interactions is not possible. However, simultaneous tuning is possible with optical Feshbach resonances (OFR) when the resonant frequencies of the boson-boson and boson-fermion interactions are well separated. In an earlier study, the possibility of simultaneous and independent tuning in the ^{40}K-^{6}Li mixture through a magnetic Feshbach resonance and rf-field-induced Feshbach resonance was examined [22]. However, such a possibility does not apply to zero electronic spin (closed-shell) atoms like Yb.

With the realization of quantum degeneracy in the mixture of ^{174}Yb-^{173}Yb where intraspecies interactions for ^{174}Yb can be tuned by OFR [23], we find it pertinent to revisit these studies. With the possibility of tuning interspecies interactions for the ^{174}Yb-^{173}Yb mixture, it may be possible to realize the ground-state geometries which are hitherto elusive. We, therefore, consider the ^{173}Yb-^{174}Yb mixture to study the density profiles for various values of coupling strengths in the present work. It must also be mentioned that the isotopes of Yb exhibit a wide range of inter- and intraspecies interactions. This has attracted lot of attention as selected isotopic compositions may exhibit dynamical instabilities triggered through the interactions. The ^{174}Yb-^{176}Yb mixture is one such Bose-Bose binary mixture currently investigated for instabilities on account of the attractive intraspecies interaction of ^{176}Yb [24,25].

The paper is organized into four sections. In the next section, Sec. II, we provide a brief description of the mean-field equations of bosons and fermions. This is followed with the section on phase separation, where the nature of Bose-Fermi phase separation is discussed as a function of the interspecies interaction. More importantly, the occurrence of fermion pinching is explored. Position swapping between bosons and fermions, as the interspecies interaction is increased, is then examined in the next section. We then conclude with Sec. V.

II. ZERO-TEMPERATURE MEAN-FIELD DESCRIPTION

We examine the stationary state properties of a Bose-Fermi (BF) mixture consisting of ^{174}Yb and ^{173}Yb in spherically symmetric trapping potentials,

$$V_{\rm B}(\mathbf{r}) = \tfrac{1}{2}m_{\rm B}\omega^2 r^2, \qquad V_{\rm F}(\mathbf{r}) = \tfrac{1}{2}m_{\rm F}\omega^2 r^2, \tag{1}$$

where the subscripts B and F stand for boson and fermion, respectively, and ω is the radial trap frequency for the two components. The fermions are spin polarized (single species) and the fermion-fermion mean-field interactions arise from the degeneracy pressure [26], whereas the boson-boson and boson-fermion interactions arise from the s-wave scattering

between the atoms. Considering these, the mean-field energy functional of the Bose-Fermi mixture is [27]

$$\begin{aligned} E[\Psi_{\rm B},\Psi_{\rm F}] &= \int d\mathbf{r}\Bigg[N_{\rm B}\left(\frac{\hbar^2|\nabla\Psi_{\rm B}|^2}{2m_B}+V_{\rm B}|\Psi_{\rm B}|^2+\frac{1}{2}G_{\rm BB}|\Psi_{\rm B}|^4\right) \\ &+N_{\rm F}\left(\frac{\hbar^2|\nabla\Psi_{\rm F}|^2}{6m_{\rm F}}+V_{\rm F}|\Psi_{\rm F}|^2+\frac{3}{5}A|\Psi_{\rm F}|^{10/3}\right) \\ &+G_{\rm BF}N_{\rm B}|\Psi_{\rm B}|^2|\Psi_F|^2\Bigg], \end{aligned} \tag{2}$$

where $\Psi_{\rm B}(\mathbf{r},t)$ and $\Psi_{\rm F}(\mathbf{r},t)$ are bosonic and fermionic wave functions satisfying the normalization condition,

$$\int d\mathbf{r}|\Psi_{\rm B}(\mathbf{r},t)|^2=\int d\mathbf{r}|\Psi_{\rm F}(\mathbf{r},t)|^2=1. \tag{3}$$

Here, $G_{\rm BB}=4\pi\hbar^2a_{\rm BB}N_{\rm B}/m_{\rm B}$, where $a_{\rm BB}$ is the bosonic s-wave scattering length and $N_{\rm B}$ is the number of bosons, is the bosonic intraspecies interaction; $G_{\rm BF}=2\pi\hbar^2a_{\rm BF}N_{\rm F}/m_R$ and $G_{\rm FB}=2\pi\hbar^2a_{\rm BF}N_{\rm B}/m_R$, where $m_R=(m_{\rm B}m_{\rm F})/(m_{\rm B}+m_{\rm F})$ is the reduced mass, $N_{\rm F}$ is the number of fermions, and $a_{\rm BF}$ is the interspecies scattering length, are the interspecies interactions, and $A=\hbar^2(6\pi^2N_{\rm F})^{2/3}/(2m_{\rm F})$. The Lagrangian of the system is

$$L=\int d\mathbf{r}\frac{i\hbar}{2}\sum_{i={\rm B,F}}\left(\Psi_i^\star\frac{\partial\Psi_i}{\partial t}-\Psi_i\frac{\partial\Psi_i^\star}{\partial t}\right)-E[\Psi_{\rm B},\Psi_{\rm F}]. \tag{4}$$

Using the action principle,

$$\delta\int_{t_1}^{t_2}Ldt=0, \tag{5}$$

we get a set of coupled partial differential equations,

$$i\hbar\frac{\partial\Psi_{\rm B}}{\partial t}=\left[-\frac{\hbar^2\nabla^2}{2m_{\rm B}}+V_{\rm B}(\mathbf{r})+G_{\rm BB}|\Psi_{\rm B}|^2+G_{\rm BF}|\Psi_{\rm F}|^2\right]\Psi_{\rm B}, \tag{6a}$$

$$i\hbar\frac{\partial\Psi_{\rm F}}{\partial t}=\left[-\frac{\hbar^2\nabla^2}{6m_{\rm F}}+V_{\rm F}(\mathbf{r})+A|\Psi_{\rm F}|^{4/3}+G_{\rm FB}|\Psi_{\rm B}|^2\right]\Psi_{\rm F}. \tag{6b}$$

The previous set of equations is valid for Bose-Fermi mixtures consisting of a Bose-Einstein condensate (BEC) and a Fermi sea of spin-polarized fermions. For superfluid Bose-Fermi mixtures, consisting of BECs of bosonic component and Cooper pairs between two different hyperfine states of fermions, the modified mean-field equation for the fermionic component (BEC of Cooper pairs) has been proposed in Refs. [28,29].

It is more convenient to rewrite Eq. (6) in a dimensionless form by defining dimensionless parameters in terms of the frequency ω and the oscillator length $a_{\rm ho}=\sqrt{\hbar/(m_{\rm B}\omega)}$. Using $\tilde{\mathbf{r}}=\mathbf{r}/a_{\rm ho}$, $\tilde{t}=t\omega$ as the scaled dimensionless variables of length and time, respectively, Eq. (6) can be rewritten as

$$i\frac{\partial\psi_{\rm B}}{\partial\tilde{t}}=\left[-\frac{\nabla_{\tilde{\mathbf{r}}}^2}{2}+V_{\rm B}(\tilde{\mathbf{r}})+g_{\rm BB}|\psi_{\rm B}|^2+g_{\rm BF}|\psi_{\rm F}|^2\right]\psi_{\rm B}, \tag{7a}$$

$$i\frac{\partial\psi_{\rm F}}{\partial\tilde{t}}=\left[-\frac{\nabla_{\tilde{\mathbf{r}}}^2}{6m_{\rm ratio}}+m_{\rm ratio}V_{\rm F}(\tilde{\mathbf{r}})+g_{\rm FF}|\psi_{\rm F}|^{4/3}+g_{\rm FB}|\psi_{\rm B}|^2\right]\psi_{\rm F}, \tag{7b}$$

where the rescaled wave functions are $\psi_{\rm B}=a_{\rm ho}^{3/2}\Psi_{\rm B}(\tilde{\mathbf{r}},\tilde{t})$ and $\psi_{\rm F}=a_{\rm ho}^{3/2}\Psi_{\rm F}(\tilde{\mathbf{r}},\tilde{t})$. Similarly, the interaction strength parameters are

$$g_{\rm BB}=\frac{4\pi a_{\rm BB}N_{\rm B}}{a_{\rm ho}},\qquad g_{\rm BF}=\frac{2\pi a_{\rm BF}N_{\rm F}}{m_R\,a_{\rm ho}},$$
$$g_{\rm FF}=\frac{(6\pi^2N_{\rm F})^{2/3}}{2m_{\rm ratio}},\qquad g_{\rm FB}=\frac{2\pi a_{\rm BF}N_{\rm B}}{m_R\,a_{\rm ho}},$$

with $m_{\rm ratio}=m_{\rm F}/m_{\rm B}$. For the sake of simplicity, we represent the scaled quantities without the tilde ($\tilde{}$) in the rest of the article. For spherically symmetric trapping potential, Eq. (6) is reduced to one-dimensional coupled mean-field equations,

$$i\frac{\partial\psi_{\rm B}}{\partial t}=\left[-\frac{1}{2}\frac{\partial^2}{\partial r^2}+\frac{r^2}{2}+g_{\rm BB}\left|\frac{\psi_{\rm B}}{r}\right|^2+g_{\rm BF}\left|\frac{\psi_{\rm F}}{r}\right|^2\right]\psi_{\rm B}, \tag{8a}$$

$$i\frac{\partial\psi_{\rm F}}{\partial t}=\left[-\left(\frac{1}{3m_{\rm ratio}}\right)\frac{1}{2}\frac{\partial^2}{\partial r^2}+m_{\rm ratio}\frac{r^2}{2}+g_{\rm FF}\left|\frac{\psi_{\rm F}}{r}\right|^{4/3}+g_{\rm FB}\left|\frac{\psi_{\rm B}}{r}\right|^2\right]\psi_{\rm F}. \tag{8b}$$

These are the coupled mean-field equations which describe the Bose-Fermi mixture in trapping potentials at zero temperature. To obtain the stationary solutions, we solve the equations numerically using the Crank-Nicholson scheme [30] with imaginary time propagation.

III. PHASE SEPARATION

Broadly speaking, for large values of $G_{\rm BB}$, the density profiles of the boson-fermion mixture in spherical symmetric traps can have three distinct geometries in the phase-separated regime: (a) fermionic core surrounded by bosonic shell, (b) bosonic core surrounded by fermionic shell, and (c) shell of bosons between fermionic core and fermionic outer shell [16]. The interspecies interactions begin to play an important role in determining the stationary state structure, when the density profiles of the bosons and fermions are of similar spatial extent. This occurs when the bosonic intraspecies interaction is strong. In the Thomas-Fermi (TF) approximation, the necessary condition for a mixture of an equal number of bosons and fermions ($N_{\rm B}=N_{\rm F}=N$) is [16]

$$a_{\rm BB}\approx 1.68m_{\rm ratio}^{-5/2}a_{\rm ho}N^{-1/6}. \tag{9}$$

The previous condition has been obtained by equating the TF radii of bosons and fermions in the absence of interspecies interaction. The condition ensures the maximum overlap between the two species in the absence of interspecies interactions and hence, accentuates the effect of switching on the interspecies interactions. Hereafter, we use $a^*_{\rm BB}$ to represent the particular value of $a_{\rm BB}$ at which bosons and fermions have the same spatial extent. For species which are isotopes of the same element the mass difference is small and $m_{\rm ratio} \approx 1$. The condition is then reduced to

$$a^*_{\rm BB} \approx 1.68 a_{\rm ho} N^{-1/6}. \tag{10}$$

Considering $N \sim 10^6$, which is the typical value in experimental realizations, $a^*_{\rm BB} \approx 0.17 a_{\rm ho}$. As $a_{\rm ho}$ is in general $\sim 10^{-6}$m for harmonic trapping potentials, the required value of $a_{\rm BB}$ is in the strongly interacting domain. It could be achieved when the interaction is tuned through a Feshbach resonance, magnetic in the case of alkali-metal atoms. With the overlapping density profiles, more intricate density patterns are observed when the interspecies interaction is increased, however, tuning $a_{\rm BF}$ with magnetic Feshbach resonance is ruled out. This complication does not arise when the interactions are tuned with well-separated OFRs, in which case, the isotopes of the two-valence lanthanide atom Yb is a suitable candidate. It has seven stable isotopes: five bosons (^{168}Yb, ^{170}Yb, ^{172}Yb, ^{174}Yb, and ^{176}Yb) and two fermions (^{171}Yb and ^{173}Yb); homonuclear OFRs of bosonic isotopes (^{172}Yb and ^{176}Yb) were recently studied [31]. Among the various possible species pairings, ^{174}Yb-^{173}Yb, which has positive intra- and interspecies background scattering lengths [32], is an ideal candidate to study Bose-Fermi mixtures in the strongly interacting domain.

For our studies, we consider a ^{174}Yb-^{173}Yb mixture containing 10^6 atoms of each species and trapped by a spherically symmetric trap with trapping frequency $\omega/(2\pi) =$ 400 Hz. The $a_{\rm BB}$ is chosen to be equal to $1100a_0$, which is achievable with the OFR of the $6s^2\ ^1S_0 \rightarrow 6s6p\ ^3P_1$ intercombination transition. And, the Bose-Fermi interspecies scattering length $a_{\rm BF}$ can be tuned with OFR of the allowed $6s^2\ ^1S_0 \rightarrow 6s6p\ ^1P_1$ transition. This is a broad line and the disadvantage of using it is high atom loss rate. However, a major advantage of OFR tuned interactions is the fine spatial control it provides. Recently, submicron modulation of scattering length using Feshback resonances was achieved in ^{174}Yb [23]. Such precise control on the spatial variation of interaction strength is unrealistic with magnetic Feshbach resonances. From here on, where it is not explicitly mentioned, reference to Bose-Fermi mixture implies the ^{174}Yb-^{173}Yb isotope mixture. To examine the density profiles of the mixture in the strongly interacting domain, we keep $a_{\rm BB}$ fixed and vary $a_{\rm BF}$ so that the system progresses from mixing to full demixing regime via partial demixing regime. It must be emphasized that with TF approximation, from Eq. (10) the spatial extent of density profiles with $a_{\rm BF} = 0$ are the same when $a^*_{\rm BB} = 1191.71a_o$ as is shown in Fig. 1(b). However, we have chosen $a_{\rm BB} = 1100a_o$, approximately the value at which the density profiles begin to exhibit the features of interest. The wave-function profiles with $a_{\rm BB} = 1100a_o$ in the absence of interspecies interactions are shown in Fig. 1(a).

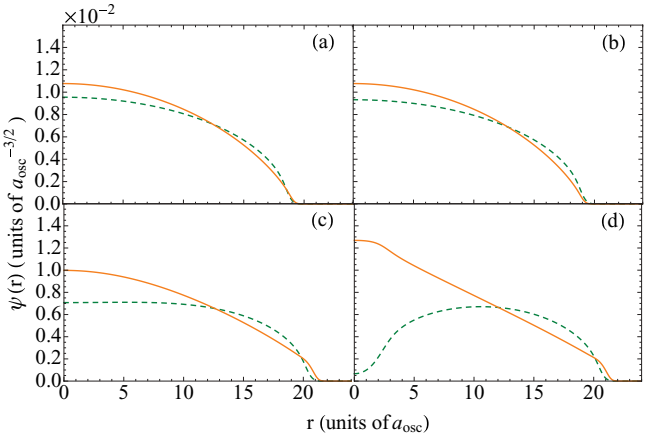

FIG. 1. (Color online) Wave-function profiles of ^{174}Yb (dashed green line) and ^{173}Yb (solid orange line) in a mixture of ^{174}Yb-^{173}Yb with $N_{\rm B} = N_{\rm F} = 10^6$, $\omega/(2\pi) = 400$ Hz and $a_{\rm BB} = 1100a_0$ as $a_{\rm BF}$ is changed from mixing to partial demixing domain. (a) For $a_{\rm BF} = 0.0$, (b) for $a_{\rm BF} = 0.0a_{\rm BB}$ and $a_{\rm BB} = 1197.11a_0$, (c) for $a_{\rm BF} = 0.6a_{\rm BB}$, and (d) for $a_{\rm BF} = 0.7a_{\rm BB}$.

A. Mixing to partial demixing regime

Starting from the initial conditions of the mixture, which as mentioned earlier has equal spatial extent of the component species and $a_{\rm BF} \approx 0$, the value of $a_{\rm BF}$ is increased. To analyze the evolution of density profiles, consider the TF profile of the bosons and fermions in scaled units as defined earlier,

$$n_{\rm F}(r) = \frac{1}{6\pi^2}\{2m_{\rm ratio}[E_{\rm F} - V_{\rm F}(r) - u_{\rm FB}n_{\rm B}(r)]\}^{3/2}, \tag{11a}$$

$$n_{\rm B}(r) = \frac{1}{u_{\rm BB}}[\mu - V_{\rm B}(r) - u_{\rm BF}n_{\rm F}(r)], \tag{11b}$$

where $u_{\rm XY} = g_{\rm XY}/N_{\rm Y}$ and $E_{\rm F}$ is the Fermi energy. From these expressions, the densities at the origin in the absence of interspecies interaction are

$$n_{\rm F}(0) = \frac{1}{6\pi^2}(2m_{\rm ratio}E_{\rm F})^{3/2}, \tag{12a}$$

$$n_{\rm B}(0) = \frac{\mu}{u_{\rm BB}}. \tag{12b}$$

In TF approximation, the Fermi energy and chemical potential of the two species are

$$E_{\rm F} = (6N)^{1/3}, \tag{13a}$$

$$\mu = \tfrac{1}{2}(15a_{\rm BB}N)^{2/5}. \tag{13b}$$

Using these in Eq. (12), the ratio of the densities at the origin is

$$\frac{n_{\rm F}(0)}{n_{\rm B}(0)} = 0.76a_{\rm BB}^{3/5}(15N)^{1/10}.$$

Consider $a_{\rm BB} \approx 0.17$, the value at which the profiles of the two species match for $N = 10^6$. The population ratio at the origin is then

$$\frac{n_{\rm F}(0)}{n_{\rm B}(0)} \approx 1.35. \tag{14}$$

that is, when $a_{\rm BF} = 0$ the fermion density is higher than the boson density at the center of the trap. Given this as the initial condition, when the interspecies interaction is switched on, the

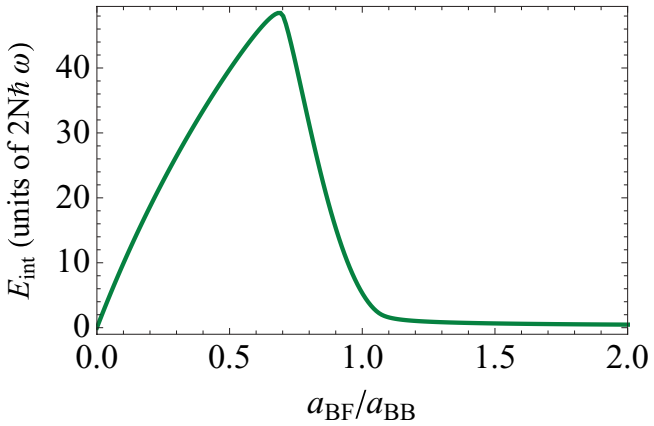

FIG. 2. (Color online) Interspecies interaction energy $E_{\rm int}$ between ^{174}Yb (boson) and ^{173}Yb (fermion) as a function of $a_{\rm BF}$. The maxima of $E_{\rm int}$ occurs at $a_{\rm BF} = 0.7a_{\rm BB}$.

interspecies mean-field energy $G_{\rm BF}|\Psi_{\rm F}(0)|^2 > G_{\rm FB}|\Psi_{\rm B}(0)|^2$. Hence, it is energetically favorable to shift the bosons from the center toward the edge of the trap. This is evident in the numerically obtained density profiles shown in Fig. 1(a), where the density profile of the bosons is flattened around the origin and has higher density at the edges.

The interspecies interaction energy in the mixing regime is

$$E_{\rm int} = \int d\mathbf{r} u_{\rm BF} n_{\rm B} n_{\rm F}, \approx \frac{3u_{\rm BF}N^2}{4\pi R_{\rm TF}^3}, \tag{15}$$

where we have used $n_{\rm B} \approx n_{\rm F} \approx N/(4\pi R_{\rm TF}^3/3)$ [21] with $R_{\rm TF} = \sqrt{2(6N)^{1/3}}$ for the system considered in the present work. As $a_{\rm BF}$ is increased further, the system enters the partial demixing regime and the characteristic signature of which is a maxima in interspecies interaction energy. For our present calculations, the variation of the interspecies interaction energy with $a_{\rm BF}$ is shown in Fig. 2. The condition for attaining partial demixing in spherical traps is [21]

$$a_{\rm BF} \geqslant \left(c_1 \frac{N_{\rm F}^{1/2}}{N_{\rm B}^{2/5}} + c_2 \frac{N_{\rm B}^{2/5}}{N_{\rm F}^{1/3}} \right) a_{\rm BB}, \tag{16}$$

where

$$c_1 = \frac{15^{3/5}}{48^{1/2}} \frac{m_{\rm F}^{3/2}}{2m_R m_{\rm B}^{1/2}} a_{\rm BB}^{3/5}, \tag{17}$$

and

$$c_2 = \frac{48^{1/3}}{15^{3/5}} \left(\frac{6}{\pi}\right)^{2/3} \frac{m_{\rm B}}{2m_R} a_{\rm BB}^{2/5}. \tag{18}$$

The previous condition for partial demixing is evaluated using TF approximation for the density profiles of both the components. From Eq. (16), the critical value of $a_{\rm BF}$ required to reach the partial demixing regime for the Bose-Fermi mixture under consideration is $0.44a_{\rm B}$ and is significantly lower than the value of $0.7a_{\rm BB}$ obtained from the numerical solution of the coupled mean-field equations [Eq. (8)]. The difference may be attributed to the simplifying assumptions in deriving the location of the interspecies interaction energy extrema, one of which is choosing the density profiles at $a_{\rm BF} = 0$ to calculate the interspecies interaction energy. At $a_{\rm BF} = 0.7a_{\rm BB}$ there is dramatic decrease in the density of the bosons near the trap center. This is accompanied by a corresponding decrease in the overlap region between the two components as is shown in Fig. 1(d).

B. Partial demixing to phase separation

A further increase of $a_{\rm BF}$, beyond the critical value, enhances the segregation of the two species. This lowers the interspecies overlap and balances the larger interaction energy from higher $a_{\rm BF}$. Ultimately, at higher values of $a_{\rm BF}$ the overlap is almost zero; the system can then be considered fully phase separated. The condition to attain phase separation or a fully demixed regime is [21]

$$\alpha k_{\rm F} a_{\rm BB} > \left(\frac{a_{\rm BB}}{a_{\rm BF}}\right)^2, \tag{19}$$

where

$$k_{\rm F} = (48N_{\rm F})^{1/6}, \quad \text{and} \quad \alpha = \frac{3^{1/3}}{4(2\pi)^{2/3}} \frac{m_{\rm B}m_{\rm F}}{m_R^2}. \tag{20}$$

For the ^{174}Yb-^{173}Yb mixture with the previously mentioned parameters, the aforementioned criterion translates into $a_{\rm BF} > 0.9a_{\rm BB}$. In the phase-separated domain, the separation occurs around the inner point where densities are equal. To identify the location of this point, consider the $a_{\rm BF} = 0$ density profiles. If the two profiles intersect at $r_{\rm i}$, then from the TF approximation $r_{\rm i}$ is the solution of the equation,

$$\{2m_{\rm ratio}[E_{\rm F} - V_{\rm F}(r_{\rm i})]\}^3 = \left(\frac{6\pi^2}{u_{\rm BB}}\right)^2 [\mu - V_{\rm B}(r_{\rm i})]^2. \tag{21}$$

For the system of our interest, $V_{\rm F}$ and $V_{\rm B}$ are almost identical. Furthermore, when $a_{\rm BB}$ is chosen [it satisfies Eq. (10)] to match the spatial extents of the densities, $E_{\rm F} \approx \mu$, following which, to a very good approximation $[E_{\rm F} - V_{\rm F}(r_{\rm i})] \approx [\mu - V_{\rm B}(r_{\rm i})]$. The solution of Eq. (21) is then

$$r_{\rm i} = \left[2E_{\rm F} - \frac{1}{4m_{\rm ratio}^3}\left(\frac{6\pi^2}{u_{\rm BB}}\right)^2\right]^{1/2}. \tag{22}$$

The importance of $r_{\rm i}$ is for the following: $n_{\rm F}(r) > n_{\rm B}(r)$ for $r < r_{\rm i}$, and $n_F(r) < n_{\rm B}(r)$ for $r > r_{\rm i}$. For the ^{174}Yb-^{173}Yb mixture, based on the previous relation $r_{\rm i} = 13.09a_{\rm ho}$ for $N_{\rm B} = N_{\rm F} = 10^6$ and $a_{\rm BB} = 0.17a_{\rm ho}$, while the numerical value is $r_{\rm i} = 12.42a_{\rm ho}$. Energetically, when $a_{\rm BF}$ is switched on it is favorable to accommodate the bosons and fermions at the outer and inner regions about $r_{\rm i}$, respectively. As $a_{\rm BF}$ is increased, the position of $r_{\rm i}$ tends to migrate outward but not dramatically.

With further increase in $a_{\rm BF}$, the bosons are expelled toward the edge of the trapping potential while the fermions are squeezed toward the trap center (see Fig. 3). With TF approximation, the effective potential experienced by ^{173}Yb in the overlap region is

$$V_{\rm eff} = \left(m_{\rm ratio} - \frac{g_{\rm BF}}{g_{\rm BB}}\right)\frac{r^2}{2} \approx \left(1 - \frac{g_{\rm BF}}{g_{\rm BB}}\right)\frac{r^2}{2}, \tag{23}$$

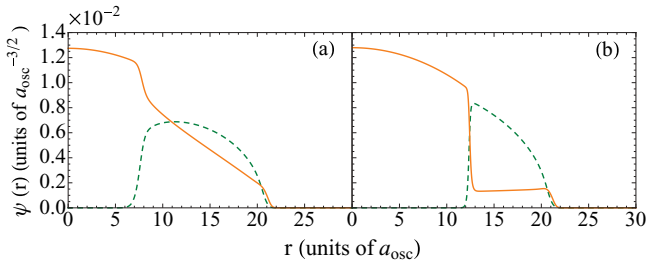

FIG. 3. (Color online) The wave-function profiles of ^{174}Yb (dashed green line) and ^{173}Yb (solid orange line) in a mixture of ^{174}Yb-^{173}Yb, with $N_B = N_F = 10^6$, $a_{BB} = 1100a_0$, and $\omega/(2\pi) =$ 400 Hz. (a) $a_{BF} = 0.75a_{BB}$ and (b) $a_{BF} = 1.0a_{BB}$.

where we have considered $m_{ratio} \approx 1$ for the ^{174}Yb-^{173}Yb mixture. Obviously, the effective potential experienced by fermions vanishes at $a_{BF} = a_{BB}$, and this explains the constant wave-function profile of ^{173}Yb in the overlap region as is shown in Fig. 3(b). Unlike two-component BECs, the density of the fermions in the region occupied by bosons is not zero when the criterion for full demixing is satisfied.

C. Fermion pinching

For the values of a_{BB} marginally below a^*_{BB}, besides r_i there is another point r_o where the densities are identical as is evident from Fig. 1(a). The location of r_o is rather sensitive to kinetic energy corrections of the bosons [33],

$$E_{kin} = 2.5\frac{N_B}{R^2_{TF}}\ln\left(\frac{R_{TF}}{1.3}\right). \tag{24}$$

Without the kinetic energy correction, that is, with TF approximation, r_o exists up to higher values of a_{BF}. However, the kinetic energy correction softens the profile at the edges and r_o vanishes as a_{BB} approaches a^*_{BB} [see Fig. 1(b)]. In the phase-separated domain when r_o is close to the edge, the fermion density is depleted at $r_i < r < r_o$ for higher a_{BF}, and, there is fermion density enhancement at $r < r_i$ and $r > r_o$. For the bosons it is the opposite: there is density enhancement at $r_i < r < r_o$, and depletion at $r < r_i$ and $r > r_o$.

As a_{BF} is increased to values larger than a_{BB}, the effective potential within the overlap region ($r_i < r < r_o$) is approximately

$$V_{eff} \approx \mu\frac{g_{BF}}{g_{BB}} - \eta\frac{r^2}{2}, \tag{25}$$

where $\eta = |m_{ratio} - g_{BF}/g_{BB}|$ and, like in the previous case, we can take $m_{ratio} \approx 1$. The form of V_{eff} is repulsive with a maxima at r_i and decreases toward r_o. The net effect is that the fermion density profile is pinched in the region where r is marginally larger than r_i. Onset of pinching is clearly discernible in Fig. 4(a), and it is more pronounced in Fig. 4(b). At higher values of a_{BF} the pinching is complete and an island of fermions appears at the edge. Figures 4(c) and 4(d) show the formation of the fermionic island due to pinching in the ^{173}Yb-^{174}Yb mixture considered in the present work.

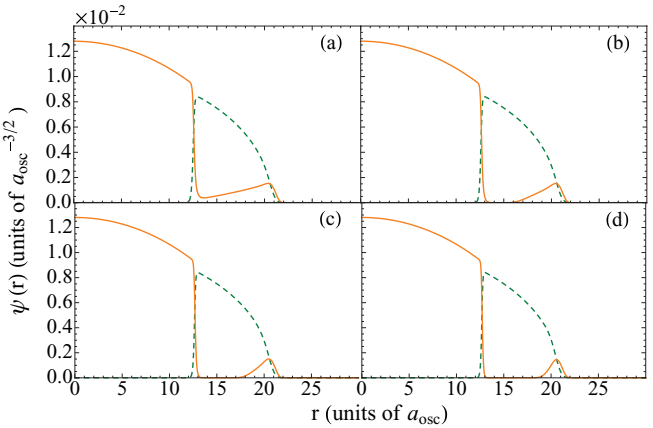

FIG. 4. (Color online) The wave-function profiles of ^{174}Yb (dashed green line) and ^{173}Yb (solid orange line) in a mixture of ^{174}Yb-^{173}Yb, with $N_B = N_F = 10^6$, $a_{BB} = 1100a_0$, and $\omega/(2\pi) =$ 400Hz, as a_{BF} is steadily increased from an initial value of $a_{BF} = a_{BB}$. (a) $a_{BF} = 1.05a_{BB}$; (b) $a_{BF} = 1.1a_{BB}$; (c) $a_{BF} = 1.15a_{BB}$; (d) $a_{BF} = 1.25a_{BB}$.

IV. PROFILE SWAPPING

A remarkable feature in the evolution of density profiles as a function of a_{BF} is the observation of profile swapping for a certain range of parameters, in which the fermions are initially at the core and bosons form a shell. However, at higher values of a_{BF} the bosons occupy the core and fermions form a shell around it.

As an example to illustrate profile swapping, consider $N_B = N_F = 10^5$; from Eq. (10) the spatial extents are equal at $a_{BB} = 0.24a_{ho}$. However, retain the value $a_{BB} = 1100a_o$ as in the case of 10^6 atoms in each species. In this case, the spatial extent of the bosons is less than the fermions, however, there are two points at which the densities of the bosons and fermions are the same. When a_{BF} is set to a nonzero value, at lower values, the changes in the equilibrium density profiles exhibit a pattern similar to fermion *pinching*. Like in fermion *pinching*, as a_{BF} is ramped up, there is a depletion of fermions from the overlap region as shown in Figs. 5(a)–5(d). However, at some value of a_{BF} a dramatic departure occurs. The fermions from the core are expelled to the edges and bosons settle at the core (Fig. 6). At intermediate values of a_{BF}, the bosons form a shell sandwiched between fermions at the core and an outer shell. This is evident from the density profiles shown in Fig. 5(d). As is evident from the figures, the migration of the fermions to the flanks occurs at a relatively minute change in a_{BF}, from $1.15a_{BB}$ to $1.16a_{BB}$.

To analyze the profile swapping based on total energy considerations, take the density profiles just prior to the expulsion of fermions from the core. The interspecies interaction energy is

$$E_{int} \approx \int_{r_i-\delta}^{r_i+\delta} d\mathbf{r} u_{BF} n_B n_F + \int_{r_i+\delta}^{\infty} d\mathbf{r} u_{BF} n_B n_F. \tag{26}$$

Here, r_i, like defined earlier, is the inner point where the two densities are equal. The first term is the interspecies interaction energy arising from the inner boundary of the overlap region. And δ is the interpenetration depth considered symmetric for simplicity. The second term is the interaction energy from

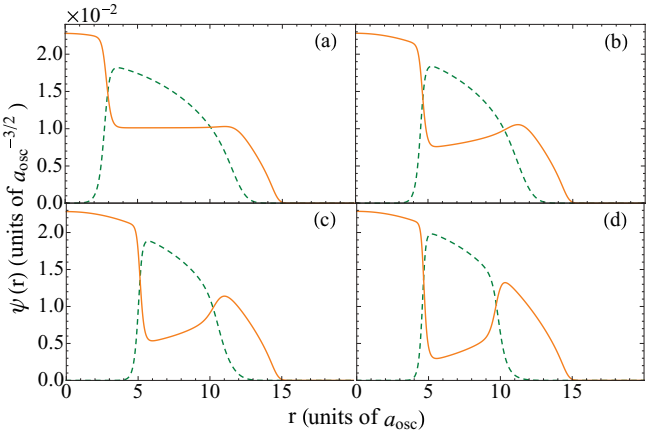

FIG. 5. (Color online) The wave-function profiles of ^{174}Yb (dashed green line) and ^{173}Yb (solid orange line) in a mixture of ^{174}Yb-^{173}Yb, with $N_B = N_F = 10^5$, $a_{BB} = 1100a_0$, and $\omega/(2\pi) = 400$ Hz, as a_{BF} is steadily increased from an initial value of $a_{BF} = a_{BB}$. (a) $a_{BF} = 1.0a_{BB}$; (b) $a_{BF} = 1.05a_{BB}$; (c) $a_{BF} = 1.1a_{BB}$; (d) $a_{BF} = 1.15a_{BB}$.

the remaining overlap region. Although the upper limit of integration is taken as ∞, in reality it extends up to the point where n_B is nonzero. To simplify the analysis, assume that the fermions from the core, after the position swapping, are pushed beyond the overlap domain. The interaction energy when swapping occurs is

$$E_{\rm int} \approx \int_0^{r_i+\delta} d\mathbf{r} u_{BF} n_B n_F + \int_{r_i+\delta}^{\infty} d\mathbf{r} u_{BF} n_B n_F, \qquad (27)$$

where in the first term, the lower limit accounts for the nonzero fermion density around the core. The occurrence of position swapping implies that

$$\int_{r_i-\delta}^{r_i+\delta} d\mathbf{r} u_{BF} n_B n_F > \int_0^{r_i+\delta} d\mathbf{r} u_{BF} n_B n_F, \qquad (28)$$

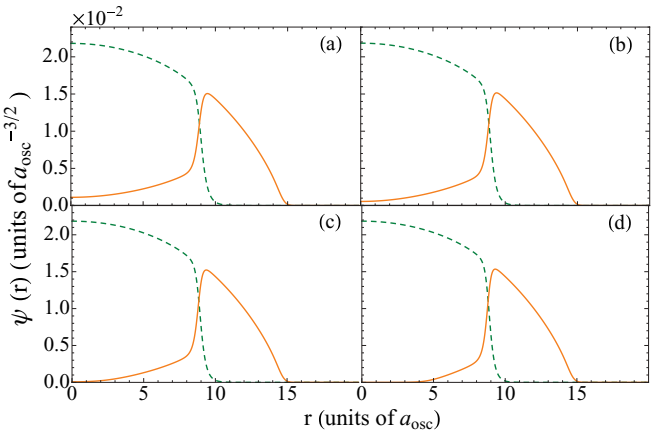

FIG. 6. (Color online) The wave-function profiles of ^{174}Yb (dashed green line) and ^{173}Yb (solid orange line) in a mixture of ^{174}Yb-^{173}Yb, with $N_B = N_F = 10^5$, $a_{BB} = 1100a_0$, and $\omega/(2\pi) = 400$ Hz, as a_{BF} is steadily increased from its initial value of $a_{BF} = 1.16a_{BB}$. (a) $a_{BF} = 1.16a_{BB}$; (b) $a_{BF} = 1.17a_{BB}$; (c) $a_{BF} = 1.18a_{BB}$; (d) $a_{BF} = 1.2a_{BB}$.

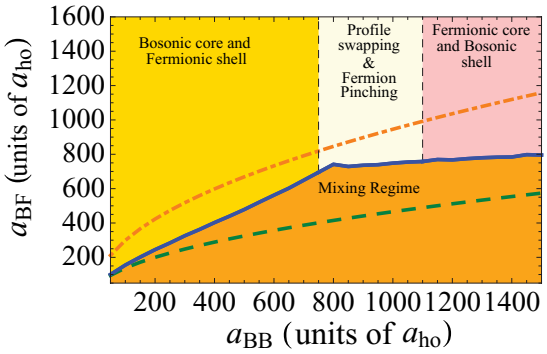

FIG. 7. (Color online) The phase diagram of the ^{174}Yb-^{173}Yb mixture with $N_B = N_F = 10^6$ and $\omega/(2\pi) = 400$ Hz. Dashed (green) and dash-dotted (orange) curves are the semianalytic conditions for mixing to partial demixing and demixing to phase separation (or full demixing) transitions respectively, while solid (blue) is the numerically obtained criterion for mixing to partial demixing transition. In the phase-separated regime, for $a_{BB} \lesssim 750$, bosonic core is surrounded by fermionic shell; for $750 \lesssim a_{BB} \lesssim 1100$ there is fermion pinching along with profile swapping at $a_{BB} \approx 750$. For $750 \lesssim a_{BB} \lesssim 1100$, bosonic shell is surrounded by fermionic core and shell. For $a_{BB} \gtrsim 1100$, fermionic core is surrounded by bosonic shell.

at some value of a_{BF}. In other words, like in binary mixtures of condensates, at some point the geometry of the overlap region determines the nature of the density profile.

To illustrate the various geometries discussed as a function of a_{BB} and a_{BF}, the phase diagram of the ^{174}Yb-^{173}Yb mixture with with $N_B = N_F = 10^6$ and $\omega/(2\pi) = 400$ Hz is shown in Fig. 7. From the figure, it is evident that the fermion pinching and profile swapping occur across a strip of parameter space. The parameter space lies between the domains of bosonic core and fermionic core. Among the different possible geometries, profile swapping initiated by tuning interspecies scattering length, appears to be a promising tool to study the Rayleigh-Taylor type of instability in Bose-Fermi mixtures. Recently, Rayleigh-Taylor instability in two-species Bose-Einstein condensates has been studied theoretically [34,35]. For degenerate Bose-Fermi mixtures, the idea is to start with a ground-state geometry with fermions forming the core, and then increase a_{BF} so that the new ground state has the fermionic core swapped by the bosonic one.

V. CONCLUSIONS

We have analyzed the equilibrium density profiles of the ^{174}Yb-^{173}Yb Bose-Fermi mixture for a range of interaction strengths. In this Bose-Fermi mixture, it is possible to tune both the Bose-Bose and Bose-Fermi interactions across a range of values. Density profiles of the two species display pinching and position swapping when the boson-boson scattering length is close to a^*_{BB}, the value at which the spatial extent of the bosons is the same as the fermions. Pinching occurs when the a_{BB} is marginally below a^*_{BB}; at these values, as a_{BF} is increased, fermions at the edges are pinched to form a thin shell, whereas at even lower values of a_{BB}, as a_{BF} is increased, the fermions are expelled to the edge and density profiles are swapped. At intermediate values of a_{BF}, the profiles undergo a series of configurations, and these are significantly different from the

ones in the Bose-Bose mixtures. Close to the profile-swapping domain, it should be possible to initiate Rayleigh-Taylor instability through a controlled variation of a_{BF}. This would be significantly different from Rayleigh-Taylor instability in condensates. In the future, it would be interesting and important to explore various instabilities which may occur at the Bose-Fermi interface boundaries. These could be qualitatively different from their analogs of binary condensates.

ACKNOWLEDGMENTS

We thank S. A. Silotri, B. K. Mani, and S. Chattopadhyay for very useful discussions. The numerical computations reported in the paper were done on the 3 TFLOPs cluster at Physical Research Laboratory. The work of P.M. is part of a research project sponsored by the Department of Science and Technology (DST), Government of India.

[1] A. G. Truscott, K. E. Strecker, W. I. McAlexander, G. B. Partridge, and R. G. Huletdagger, Science **291**, 2570 (2001).
[2] F. Schreck, L. Khaykovich, K. L. Corwin, G. Ferrari, T. Bourdel, J. Cubizolles, and C. Salomon, Phys. Rev. Lett. **87**, 080403 (2001).
[3] Z. Hadzibabic, C. A. Stan, K. Dieckmann, S. Gupta, M. W. Zwierlein, A. Görlitz, and W. Ketterle, Phys. Rev. Lett. **88**, 160401 (2002).
[4] G. Roati, F. Riboli, G. Modugno, and M. Inguscio, Phys. Rev. Lett. **89**, 150403 (2002).
[5] C. Silber, S. Günther, C. Marzok, B. Deh, Ph. W. Courteille, and C. Zimmermann, Phys. Rev. Lett. **95**, 170408 (2005).
[6] J. M. McNamara, T. Jeltes, A. S. Tychkov, W. Hogervorst, and W. Vassen, Phys. Rev. Lett. **97**, 080404 (2006).
[7] T. Fukuhara, S. Sugawa, Y. Takasu, and Y. Takahashi, Phys. Rev. A **79**, 021601(R) (2009).
[8] M. K. Tey, S. Stellmer, R. Grimm, and F. Schreck, Phys. Rev. A **82**, 011608 (2010).
[9] G. Modugno, G. Roati, F. Riboli, F. Ferlaino, R. J. Brecha, and M. Inguscio, Science **297**, 2240 (2002).
[10] F. Ferlaino *et al.*, Phys. Rev. A **73**, 040702(R) (2006); S. Inouye, J. Goldwin, M. L. Olsen, C. Ticknor, J. L. Bohn, and D. S. Jin, Phys. Rev. Lett. **93**, 183201 (2004).
[11] M. Zaccanti, C. DErrico, F. Ferlaino, G. Roati, M. Inguscio, and G. Modugno, Phys. Rev. A **74**, 041605(R) (2006).
[12] M. Modugno, F. Ferlaino, F. Riboli, G. Roati, G. Modugno, and M. Inguscio, Phys. Rev. A **68**, 043626 (2003).
[13] S. K. Adhikari, Phys. Rev. A **70**, 043617 (2004).
[14] D. C. E. Bortolotti, A. V. Avdeenkov, and J. L. Bohn, Phys. Rev. A **78**, 063612 (2008).
[15] S. Tojo, Y. Taguchi, Y. Masuyama, T. Hayashi, H. Saito, and T. Hirano, Phys. Rev. A **82**, 033609 (2010).
[16] K. Molmer, Phys. Rev. Lett. **80**, 1804 (1998).
[17] N. Nygaard and K. Molmer, Phys. Rev. A **59**, 2974 (1999).
[18] A. Minguzzi and M. P. Tosi, Phys. Lett. A **268**, 142 (2000).
[19] R. Roth, Phys. Rev. A **66**, 013614 (2002).
[20] L. Viverit, C. J. Pethick, and H. Smith, Phys. Rev. A **61**, 053605 (2000).
[21] Z. Akdeniz, A. Minguzzi, P. Vignolo, and M. P. Tosi, Phys. Rev. A **66**, 013620 (2002).
[22] P. Zhang, P. Naidon, and M. Ueda, Phys. Rev. Lett. **103**, 133202 (2009).
[23] R. Yamazaki, S. Taie, S. Sugawa, and Y. Takahashi, Phys. Rev. Lett. **105**, 050405 (2010).
[24] K. Kasamatsu and M. Tsubota, J. Low Temp. Phys. **150**, 599 (2008).
[25] G. K. Chaudhary and R. Ramakumar, Phys. Rev. A **81**, 063603 (2010).
[26] D. A. Butts and D. S. Rokhsar, Phys. Rev. A **55**, 4346 (1997).
[27] P. Capuzzi, A. Minguzzi, and M. P. Tosi, Phys. Rev. A **67**, 053605 (2003).
[28] S. K. Adhikari and L. Salasnich, Phys. Rev. A **78**, 043616 (2008).
[29] S. K. Adhikari, Phys. Rev. A **79**, 023611 (2009).
[30] P. Muruganandam and S. K. Adhikari, Comput. Phys. Commun. **180**, 1888 (2009).
[31] K. Enomoto, K. Kasa, M. Kitagawa, and Y. Takahashi, Phys. Rev. Lett. **101**, 203201 (2008).
[32] M. Kitagawa *et al.*, Phys. Rev. A **77**, 012719 (2008).
[33] F. Dalfovo, L. Pitaevskii, and S. Stringari, Phys. Rev. A **54**, 4213 (1996).
[34] S. Gautam and D. Angom, Phys. Rev. A **81**, 053616 (2010).
[35] K. Sasaki, N. Suzuki, D. Akamatsu, and H. Saito, Phys. Rev. A **80**, 063611 (2009).